Hindawi
Journal of Advanced Transportation
Volume 2023, Article ID 6682699, 10 pages
https://doi.org/10.1155/2023/6682699

Research Article

Vibration Analysis of Traction Drive System Components Based on the Field Test for High-Speed Train

Pingbo Wu,[1] Chunyuan Song,[1,2] Xun Wang,[1] Sheng Qu,[1] and Hao Wu[3]

[1]*State Key Laboratory of Rail Transit Vehicle System, Southwest Jiaotong University, Chengdu, China*
[2]*CRRC Changchun Railway Vehicles Co., Ltd., Changchun, China*
[3]*College of Mechanical and Vehicle Engineering, Chongqing University, Chongqing, China*

Correspondence should be addressed to Xun Wang; wxptf0323@my.swjtu.edu.cn and Sheng Qu; 626193245@qq.com

Received 28 May 2023; Revised 7 August 2023; Accepted 28 September 2023; Published 14 October 2023

Academic Editor: Francesco Galante

The traction drive system of a high-speed train is the key subsystem of a high-speed train, which controls the driving and braking of the train through electromechanical coupling, and determines the running speed, power quality, and comfort of the train. The traction drive system is subjected to many internal and external excitation sources and frequency bandwidth, and the dynamic response and dynamic characteristics of the system are extremely complex. The results of the traction motor field vibration test showed that 100 Hz vibration frequency occurred during traction and braking of high-speed trains when the inverter output voltage frequency was close to 100 Hz, and its vibration amplitude was higher than other frequency bands. When traction power was cut-off, the 100 Hz frequency was not significant. Through simulation analysis of fatigue damage, it was found that 100 Hz DC-link voltage pulsation would aggravate the fatigue damage of the motor hanger. The line vibration test and bench test of the gearbox showed that there was a natural frequency of the gearbox at about 2500 Hz, when the meshing frequency was close to it. Thus, the resonance characteristic became significant.

1. Introduction

As an important development direction of China's railway transportation, the high-speed train is of great significance to the nation's development and social progress. As one of the core components of a high-speed train, the traction drive system is used to convert electrical energy into mechanical energy to drive the train and convert mechanical energy into electrical energy to feed back to the power grid during train braking [1]. The traction drive system as shown in Figure 1 is mainly composed of a traction transformer, traction converter, traction motor, and mechanical drive system. The pantograph receives single-phase AC from the catenary and transmits it to the traction transformer. The single-phase alternating current is input to the pulse rectifier after being depressurized by the traction transformer. The pulse rectifier rectifies the single-phase AC into DC voltage and inputs it to the traction inverter. The inverter then outputs a three-phase AC with controllable frequency to supply the three-phase asynchronous traction motor, which converts electric energy into mechanical energy, and then drives the train through the gear transmission system [2].

The traction drive system determines the running speed and traction force of a high-speed train [3]. The speed and torque of the traction motor could be regulated by the variable frequency and amplitude AC, that is, the output of the electrical system [4]. The output end of the motor could be connected to the reduction gearbox through coupling. The pinion of the gearbox is the torque input end, which could transmit the torque to the big gear on the wheelset through gear meshing, so as to change the high speed and small torque output by the traction motor into low speed and large torque, and then drive the bogie of the train. During train operation, there are abundant internal and external excitations such as electrical system harmonics, wheel-rail excitation, and gear meshing [5, 6], which directly or indirectly affect the vibration characteristics of traction drive system components.

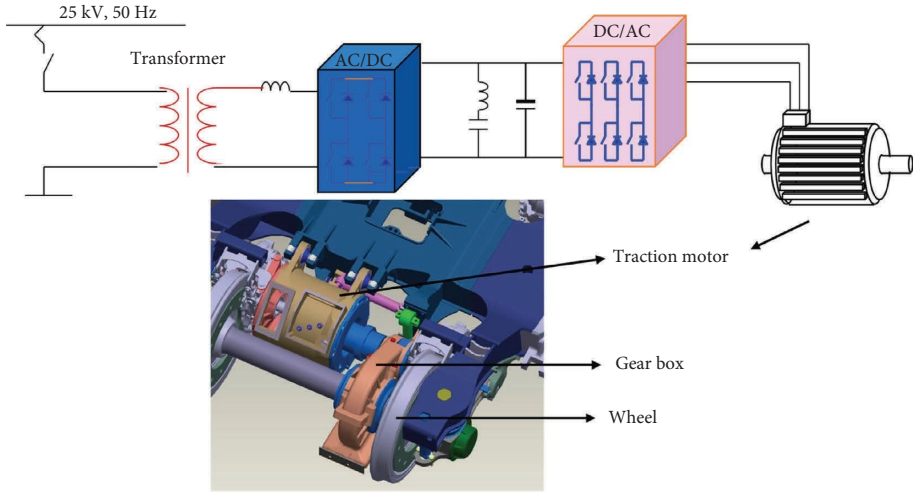

Figure 1: Schematic diagram of traction drive system for a high-speed train.

A high-speed train traction drive system has a complex transmission structure, rich nonlinear factors and internal excitation, and complex external excitation of high-speed trains [7–9]. The structural components of the traction drive system could usually work under high-frequency vibration conditions and bear periodic loads [10]. So, special attention should be paid to its vibration control and structural reliability. The high-speed trains running in China have the characteristics of long-running mileage, high use density, many long and short routes, large differences in regional climatic conditions, and complex environments along the high-speed railway [11]. When the train is running at high speed, complex random external excitation would be imposed on the traction drive system due to the coupling effects of wheel irregularity, tread scratch, peeling, welded joints on the rail surface, wave wear, and other irregularities, as well as the suspension characteristics of the bogie of the vehicle [12]. During the meshing process of the transmission gear of the traction gearbox, pitting corrosion, wear, contact fatigue, and fracture often occur due to alternating internal load, vibration, and shock on the gearbox [13].

With the large operation frequency of high-speed trains and the sharp increase in running mileage, and the intensification of wheel wear, the reliability problems of the traction drive system appeared gradually. The dynamic response and dynamic characteristics [1, 12, 14, 15] of the traction drive system could be extremely complex due to many excitation sources, frequency bandwidth, and strong coupling characteristics between external variable load excitation [16] and internal incentive and flexible supports. The internal excitation of the traction drive system mainly includes multiple pairs of meshing pair variable stiffness excitation, meshing error, and motor output torque ripple. Wang et al. [4] revealed the influence of high-frequency vibration caused by the harmonic torque of the traction motor on the bogie of rail vehicles. The influence of the time-varying stiffness of meshing teeth pairs and the gear transmission error as internal excitation of the traction system on the bogie of the high-speed train was analyzed by Huang et al. [9] through simulation and test, which did not consider the internal excitation caused by oscillation of the traction electric system. The fatigue problem of bogie caused by electrical system fluctuation was studied by Mao et al. [17] and Wu et al. [18]. Overall, the analysis of the impact of electrical signals in the traction system on the mechanical components of the transmission system mainly focuses on the impact of the pulsating torque formed by harmonics in the traction motor, which are generated by the PWM inverter. There are also a few simulation studies on the impact of 100 Hz beat frequency on the mechanical components of the transmission system, but there is a lack of complete data obtained through field tests to study the impact of 100 Hz beat frequency on the traction motor hanger. In this work, the vibration characteristics of traction drive system components could be analyzed through field tests and simulation. It is helpful for the innovative design and dynamic performance optimization of high-speed train traction drive systems under multisource excitation, as well as for the safe and reliable operation of the system.

2. Vibration Characteristics of Traction Motor

Due to the inherent characteristics of single-phase pulse rectifiers in high-speed railways, the intermediate DC voltage contains a beat frequency component which is twice the size of grid side frequency. The beat frequency component is transmitted to the traction motor through the inverter, resulting in beat frequency phenomena such as motor current and electromagnetic torque fluctuation, and abnormal vibration of the motor. According to the equivalent mathematical model of a traction rectifier, its input power is

$$P_{\text{in}} = U_s I_s \cos(\phi) + U_s I_s \cos(2\omega_s t + \phi). \tag{1}$$

The output power is

$$P_{\text{out}} = U_{\text{dc}} I_L + C_d U_{\text{dc}} \frac{\mathrm{d}u_{\text{dc}}}{\mathrm{dt}}, \tag{2}$$

where U_s is the effective value of grid side voltage, I_s is the effective value of grid side current, ω_s is the grid side angle frequency, ϕ is the phase angle of grid side current lead voltage, U_{dc} is the average value of DC side output voltage, u_{dc} is the fluctuation value of DC side output voltage, and I_L is the average value of load current.

By ignoring the loss of rectifier power devices and the equivalent impedance of transformer's secondary side, the output power is equal to the input power, and the DC side voltage ripple component could be obtained as follows:

$$u_{\mathrm{dc}} = \frac{I_L \sin(2\omega_s t + \phi)}{2\omega_s C_d \cos(\phi)}. \tag{3}$$

According to equation (3), the fluctuation frequency of pulsating voltage on the DC side is twice the electric frequency on the grid side, i.e., 100 Hz. Let $\Delta U_{\mathrm{dc}} = I_L/2\omega_s C_d \cos(\phi)$, and the actual value of DC side voltage could be rewritten as

$$u_{\mathrm{dc}} = U_{\mathrm{dc}} + \Delta U_{\mathrm{dc}} \sin(2\omega_s t + \phi). \tag{4}$$

Assuming that all switching devices of traction inverters are ideal switches, the switching function could be defined as

$$S_v(t) = \frac{1}{2} + \sum_{k=\mathrm{odd}}^{\infty} A_{\mathrm{vk}} \cos k(\omega_n t + \phi_v) \quad (v = a, b, c), \tag{5}$$

where $\phi_a = 0$, $\phi_b = -2\pi/3$, $\phi_c = 2\pi/3$, ω_n is the angular frequency of the output voltage of traction inverter.

The output phase voltage of the traction inverter is

$$u_{\mathrm{vo}} = u_{\mathrm{dc}}\left(S_v - \frac{1}{2}\right) = U_{\mathrm{dc}} \sum_{k=\mathrm{odd}}^{\infty} A_{vk} \cos k(\omega_n t + \phi_v) + \frac{\Delta U_{\mathrm{dc}}}{2} \sum_{k=\mathrm{odd}}^{\infty} A_{\mathrm{vk}} \sin[(2\omega_s \pm k\omega_n)t + \phi + k\phi_v]. \tag{6}$$

The output phase voltage of the traction inverter could have an odd harmonic component caused by the steady-state component of DC voltage and a harmonic component caused by the beat frequency component. Since the coefficient A_{vk} is inversely proportional to $k\omega_n$, that is, the higher the number of times of the beat frequency voltage component, the smaller the amplitude of the beat frequency voltage component. Therefore, the amplitude of the beat frequency voltage component with angular frequency $2\omega_s \pm \omega_n$ is the largest.

The beat frequency current in the traction motor is induced by the voltage beat frequency component of the traction inverter, and the beat frequency component vibration torque with angular frequency $2\omega_s \pm \omega_n$ is formed as follows:

$$T_d = \frac{3n_{\mathrm{p}}}{2\pi f_1} I_{2d+} E_2 \cos(2\omega_s t - \phi_d) + \frac{3n_{\mathrm{p}}}{2\pi f_1} I_{2d-} E_2 \cos(2\omega_s t + \pi - \phi_d), \tag{7}$$

where f_1 is the fundamental voltage frequency of the motor stator, n_{p} is the number of pole pairs, E_2 is the electromotive force induced by the motor, and $I_{2d\pm}$ is the reduction value of rotor current at an angular frequency of $2\omega_s \pm \omega_n$ components.

In the AC-DC-AC traction drive system, the beat frequency component with angular frequency $2\omega_s \pm \omega_n$ of the DC-link is inevitable. When the output voltage frequency of the inverter is close to 100 Hz, the amplitude of the pulsating torque is the highest. In the design of the traction drive system, two solutions are used to solve this problem, i.e., hardware filtering in parallel with LC series connection components in the DC-link or software filtering. However, if the filtering fails, the harmonic pulsation torque of the motor would increase, and transmission occurs through the mechanical transmission system to cause the motor suspension fatigue damage.

As the key equipment of the high-speed train, the traction motor completes the conversion of electrical energy and mechanical energy in the process of traction and braking, its operation performance directly affects the performance of the train. The vibration problem of traction motor [17] during operation would have an adverse impact on the service life of the motor. The traction motor is suspended on the frame through the motor hanger, as shown in Figure 2(a), so the motor hanger would be affected by torque pulsation of the traction motor. The motor hanger and traction motor are shown in Figure 2(b). If the motor vibration amplitude is too large, vibration fatigue may occur at the welding position of the motor hanger, as shown in the red circle in Figure 2(c). Internal excitations such as harmonic torque output by the traction motor and meshing of the gearbox would cause motor vibration and would transmit it to the motor hanger. The external excitation of the wheel-rail is transmitted to the frame through the primary suspension and then to the motor hanger and traction motor [19, 20].

The motor of the EMU is suspended on the frame through the leaf spring structure, which is an important part of the traction transmission system. In order to improve the safety of the leaf spring suspension structure, the field test research of the motor hanger was carried out. Through the field test, the vibration characteristics of the transmission system of the vehicle were examined. The distribution of the test points is shown in Figures 3 and 4.

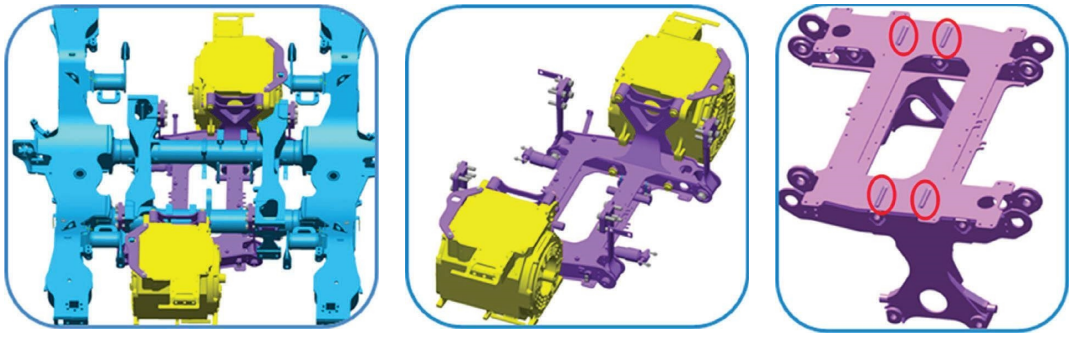

(a) (b) (c)

Figure 2: Structure of the traction motor suspension system for high-speed train: (a) motor hanger, frame, and traction motor, (b) motor hanger and traction motor, and (c) motor hanger.

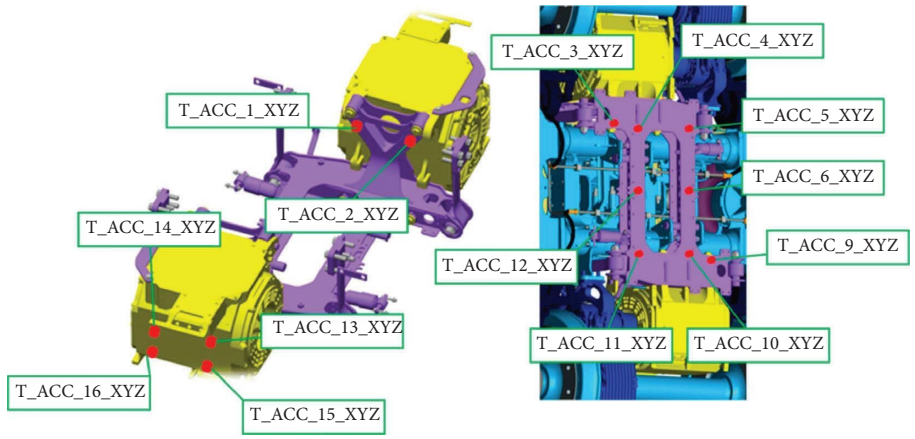

Figure 3: The distribution of test points of traction motor and motor hanger.

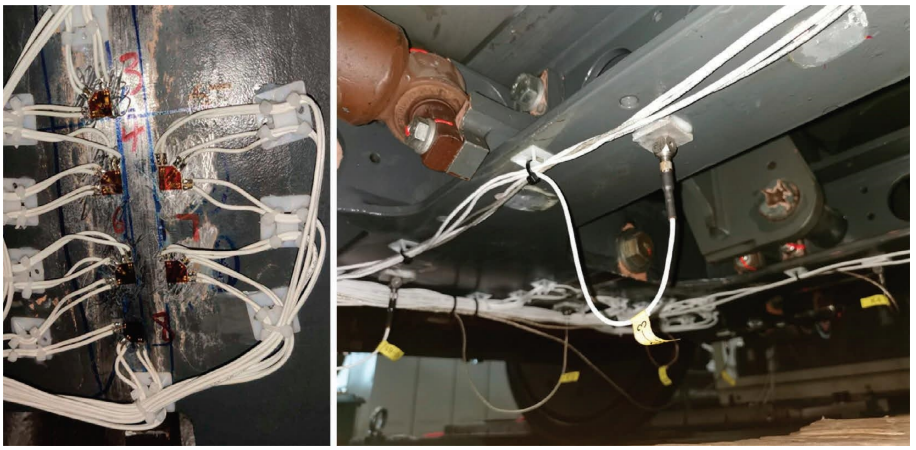

Figure 4: The layout of measuring points for the traction motor test.

The large and small gears in the gearbox would produce meshing frequency in the meshing process. During the operation of a high-speed train, the meshing frequency would increase with the increase in speed. The gear meshing frequency of the gearbox of high-speed trains is as follows:

$$f_n = f_w * n_z,$$
$$f_{w1} = \frac{v}{2\pi r}, f_{w2} = f_{w1} * a., \tag{8}$$

where f_w is the gear rotation frequency, Hz; f_{w1} is the large gear rotation frequency, Hz; f_{w2} is the pinion rotation frequency, Hz; v is the train running speed, m/s; r is the wheel radius, 0.46 m; n_z is the number of gear teeth; and a is the gear ratio, 85 : 35.

During the uniform motion of the train, small fluctuations in speed are inevitable, as well as some errors during gear operation. Therefore, the meshing frequency band was selected for data analysis, rather than a certain meshing frequency value. According to the calculation of the number of teeth of the large and small gears of the gearbox, the gear meshing frequency band was between 2400 Hz and 2600 Hz when running at 300 km/h and the gear meshing frequency band was between 1600 Hz and 1700 Hz when running at 200 km/h. The time-frequency analysis of motor vibration under three operation conditions of 300 km/h, 200 km/h traction cut-off, and 200 km/h was performed. The results showed that the contribution of meshing frequency to the vibration components of the motor was not significant. During traction and braking, there was a remarkable vibration frequency of 100 Hz in the vibration components of the traction motor when the inverter output voltage frequency was close to 100 Hz.

As shown in Figure 5(a), there was little significant vibration frequency between 2400 Hz and 2600 Hz. The vibration frequency amplitude was very small and had little impact on the transmission system. In the 0–200 Hz frequency band, it could be observed from Figure 5(b) that there is a very prominent vibration frequency of 100 Hz under the traction condition. In the whole train operation process of traction-constant speed-braking, a 100 Hz vibration frequency always existed. However, under traction conditions, when the speed was from 148 km/h to 194 km/h, the 100 Hz vibration frequency was very significant, and the vibration amplitude was far greater than that of other frequency bands. It showed that 100 Hz vibration frequency had a great impact on motor vibration, which may aggravate the fatigue damage of motor hangers.

It could be seen from Figure 6(a) that the color of the time-frequency diagram of motor vibration was green, the vibration amplitude was very small, and the meshing frequency was not significant. It could be seen from the time-frequency diagram of 200 km/h traction cut-off as shown in Figure 6(b) that the amplitude of vibration frequency below 15 Hz was greater than that of other vibration frequency bands. It indicated that the rigid body motion of the motor was relatively significant in this condition. Compared with Figure 7(b), the 100 Hz vibration frequency basically did not exist during traction cut-off, indicating that 100 Hz was a torque ripple caused by electrical signals. It showed that the 100 Hz vibration frequency was transmitted by the electrical system, causing abnormal vibration of the motor.

From Figure 7, it could be seen that in the whole 200 km/h constant speed operation process, the vibration frequency amplitude between 1600 Hz and 1750 Hz was relatively small, and the meshing frequency was not prominent. It could be seen from Figure 7(b) that the 100 Hz vibration frequency always existed during the whole operation of the high-speed train. It was worth noting that for a period of time in the process of traction and braking, the 100 Hz vibration frequency was very significant, the vibration amplitude was very large, and the amplitude of the 100 Hz vibration frequency under traction conditions was larger than that under braking conditions. Compared with Figure 5(b), under traction conditions, the amplitude of 100 Hz vibration frequency at 300 km/h was larger than that at 200 km/h.

Through comparative analysis of the abovementioned three operating conditions, it can be seen that the meshing frequency of the gear system has little effect on the vertical vibration of the motor. The 100 Hz vibration frequency is the vibration caused by the actual electrical signal during the operation of high-speed trains, which is most severe when the inverter output voltage frequency is close to 100 Hz. Based on previous theoretical analysis, this 100 Hz is the beat frequency component that exists after rectification in the traction transmission system and is filtered and processed by the DC-link. However, a significant 100 Hz vibration appeared in the vertical vibration of the traction motor field test data, indicating that the filtering effect of the DC-link may not be ideal and requires attention, otherwise it may cause fatigue damage to the motor hanger.

The time domain diagram of vibration acceleration and stress for traction motor as shown in Figure 8 was obtained after 100 Hz filtering. It could be seen from the diagram that the variation trend of stress and acceleration with time was consistent, indicating that the stress and vibration of the 100 Hz component could correspond to each other.

As shown in Figure 9(a), the three vibration frequencies were prominent, which were the fundamental component f_i and two harmonic components $f_i + 2f_{net}$ and $f_i - 2f_{net}$. Based on the motor control theory, the operation speed of the high-speed train is controlled by the fundamental frequency f_i. The other two components are current harmonics caused by the pulsating component of the $2f_{net}$ frequency of the DC-link. It could be seen that as the fundamental frequency of the current f_i approaches the DC voltage pulsation frequency $2f_{net}$, the current component of the two harmonic frequencies becomes significant. From Figure 9(b), we could observe the two vibration frequencies, $2f_{net}$ and $4f_{net}$ for the entire acceleration-uniform-deceleration process. It could be found from Figure 9 that the harmonic component of the motor electromagnetic torque was most pronounced when the fundamental frequency of the current f_i was close to the DC voltage pulsation frequency $2f_{net}$.

The rain-flow counted history of the dynamic stress could be presented in a cumulative exceedance diagram as shown in Figure 10. The overall trend showed that the stress amplitudes in the two datasets differ by two orders of magnitude. Based on the statistics, the fatigue damages of the motor hanger in two situations were calculated, as shown in Table 1, and the results indicated that the 100 Hz DC-link voltage pulsation aggravated the fatigue damage of the motor hanger [18].

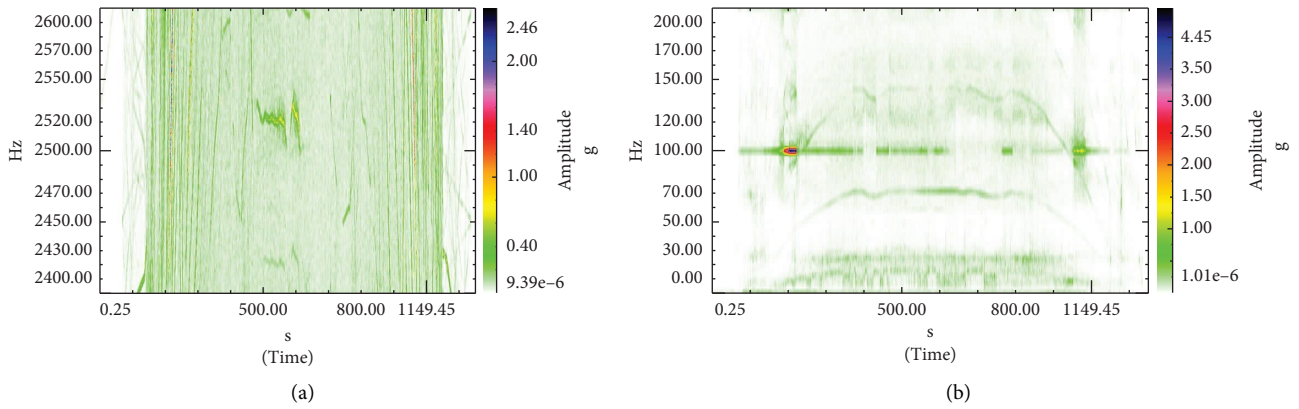

Figure 5: Time-frequency diagram of vertical vibration for motor under 300 km/h: (a) 2400 Hz–2600 Hz and (b) 0 Hz–200 Hz.

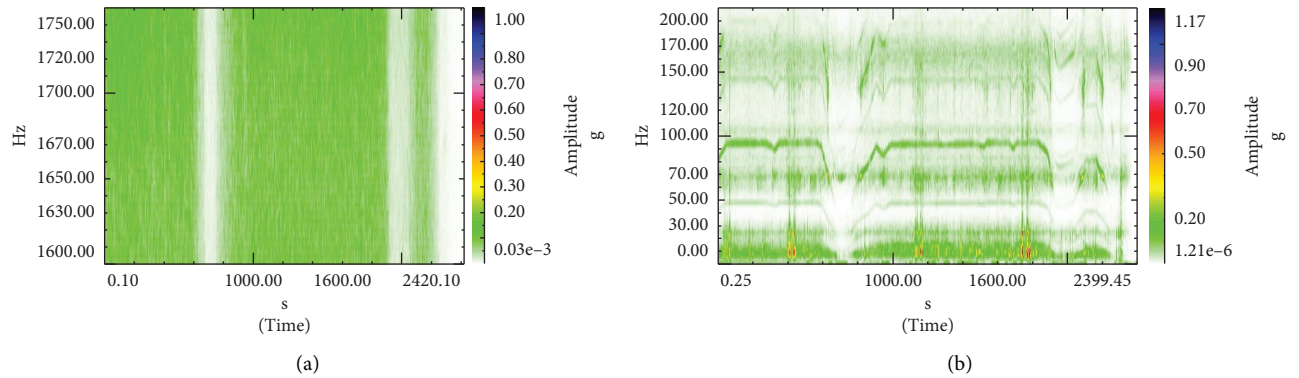

Figure 6: Time-frequency diagram of vertical vibration for motor under 200 km/h traction cut-off: (a) 1600 Hz–1750 Hz and (b) 0 Hz–200 Hz.

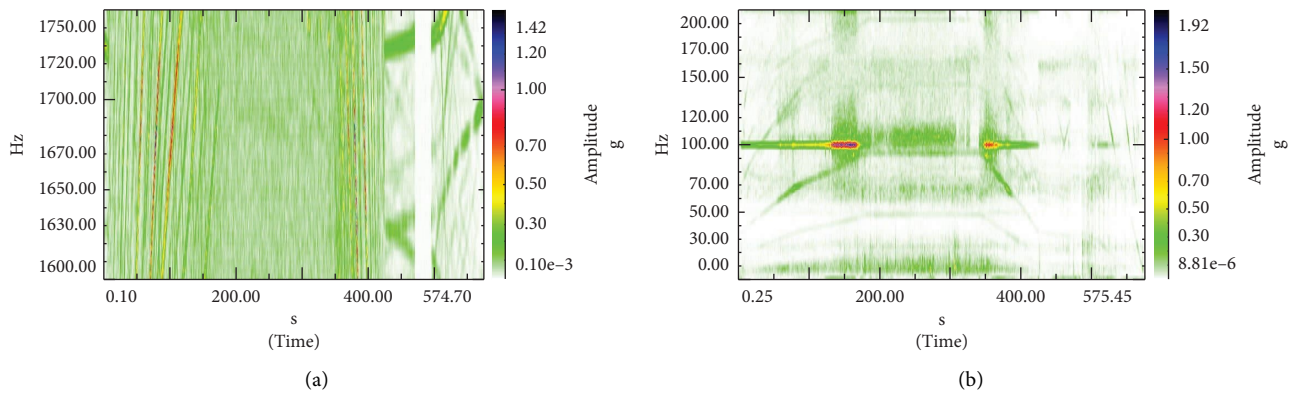

Figure 7: Time-frequency diagram of vertical vibration for motor under 200 km/h: (a) 1600 Hz–1750 Hz and (b) 0 Hz–200 Hz.

3. Vibration Characteristics of Gearbox

A high-speed train gearbox system consists of a transmission system composed of a gear pair and transmission shaft and a structural system composed of a bearing and box. It is a complex elastic mechanical system and its working performance directly determines the service safety of the train. As the carrier of the gear transmission system of a high-speed train, the gearbox must bear complex and changeable internal and external excitation loads during the high-speed operation of the train [21] including the internal excitation of periodic vibration caused by the change of gear meshing stiffness, the external excitation of wheel-rail impact caused by track irregularity and wheel wear, and the harmonic torque formed by the rotating shaft of traction motor [22–24]. Under the coupling action of these excitations, the working state of the gearbox is complex and changeable.

When the vehicle is running at 300 km/h, the gear meshing frequency band is about 2500 Hz. In order to study the influence of speed on gear meshing, the gearbox

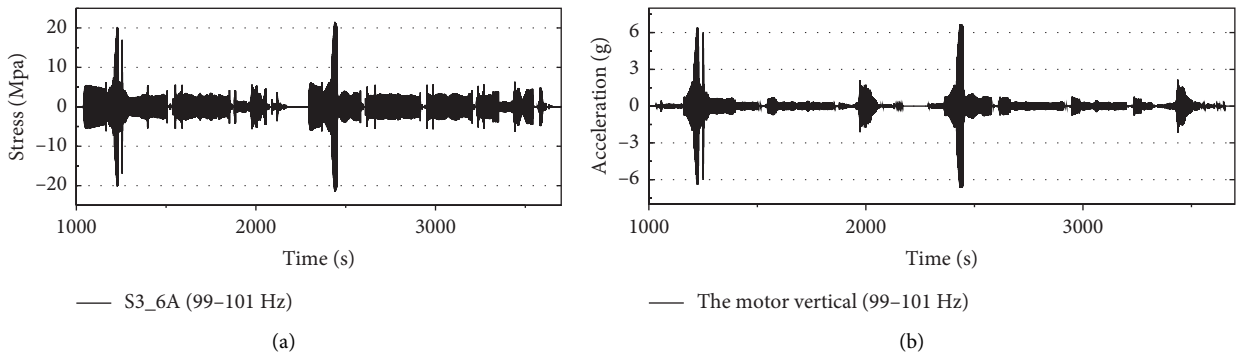

Figure 8: Time domain diagram of stress and acceleration for traction motor vibration: (a) stress and (b) acceleration.

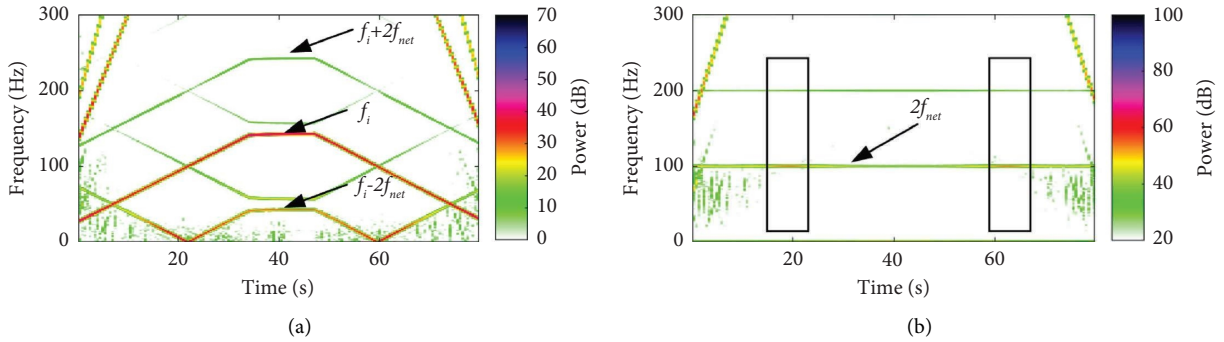

Figure 9: Simulated results with 100 Hz DC voltage pulsation for traction motor: (a) stator current spectrum and (b) torque spectrum [18].

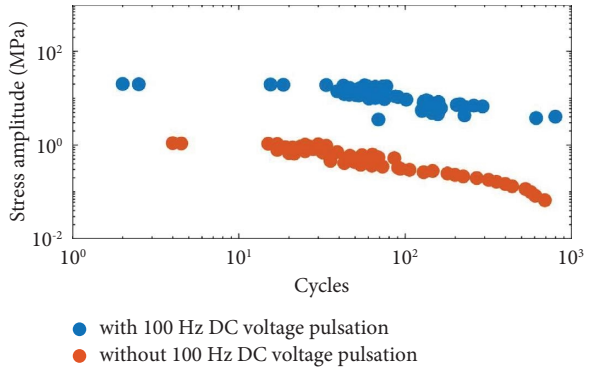

Figure 10: Cumulative exceedance diagram for motor hanger [18].

acceleration was analyzed through a 2400 Hz–2600 Hz band-pass filter. The gearbox data sampling frequency is 10000 Hz. The installation position of the gearbox measuring point is the top position of the gearbox. The time domain diagram of gearbox lateral vibration acceleration is shown in Figure 11.

2400 Hz–2600 Hz band-pass filtering was applied to lateral vibration acceleration data of the gearbox, and the time domain diagram of gearbox vibration acceleration is shown in Figure 11. Under the operation of 300 km/h, it could be observed from Figure 11 that when the speed was slightly different, the gear meshing vibration amplitude of the gearbox was significantly different. The maximum gear meshing vibration amplitude of the gearbox was 20 g at 290 km/h and its maximum vibration amplitude was 25 g at

Table 1: Fatigue damage of the motor hanger [18].

Situation	Fatigue damage
With 100 Hz DC voltage pulsation	8.30×10^{-6}
Without 100 Hz DC voltage pulsation	1.81×10^{-12}

295 km/h and 45 g from 300 km/h to 305 km/h. It could be found that the gear meshing vibration amplitude of the gearbox increased significantly with the increase of speed under the operation of 300 km/h.

It could be found from Figure 12(a) that there was a significant frequency band at about 2500 Hz, and its vibration amplitude was much larger than that of other frequency bands. The short-time Fourier of gearbox vibration acceleration at the speed of 300 km/h was locally amplified, as shown in Figure 12(b), and the vibration amplitude increased significantly when the gear meshing frequency band crossed from 2480 Hz to 2500 Hz during the rising process. It indicated that the gearbox had a natural frequency of about 2500 Hz. When the speed of a high-speed train is at 300 km/h, the gear meshing frequency of the gearbox could be close to the natural mode of the structure to form resonance, resulting in a relatively large vibration amplitude of the gearbox.

In order to further confirm whether the structural mode of the gearbox at about 2500 Hz really exists, the bench test of the ZF gearbox was carried out. The bench test speed was gradually increased from 0 km/h to 360 km/h, and the gear meshing frequency was from 0 Hz to 3030 Hz. The

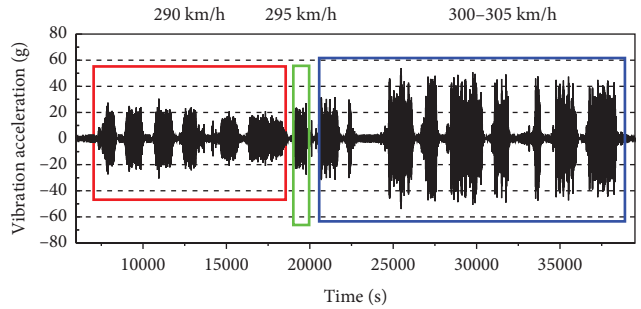

Figure 11: Lateral vibration acceleration of gearbox at 300 km/h for high-speed train.

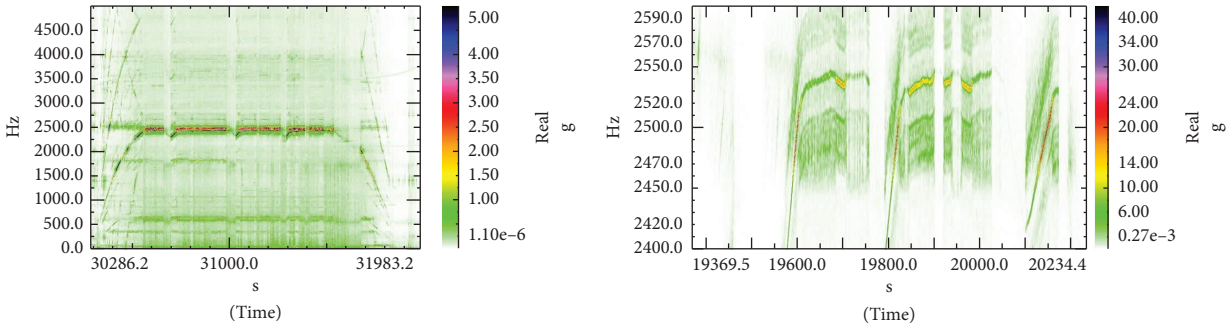

Figure 12: Time-frequency diagram of gearbox vibration acceleration at 300 km/h for a high-speed train: (a) 0–5000 Hz and (b) 2400 Hz–2600 Hz.

corresponding torque was applied during the test, and the test was carried out at two working conditions: forward rotation and reverse rotation. In order to eliminate the influence of the sensor, BK and Kistler high-frequency response sensors were pasted at the same time. Meanwhile, AB glue and 502 glue were used to eliminate the influence of bonding glue. The layout of test measuring points and some sensors is shown in Figure 13.

As can be seen from Figure 14, the vibration frequencies around 2450 Hz, 2500 Hz, and 2550 Hz were prominent, and the most significant vibration frequency was 2516 Hz. Compared with Figure 15, the same Kistler sensor was bonded with AB glue and 502 glue, respectively, to test gearbox vibration, and the vibration amplitude of the gearbox was similar and the frequency characteristics were nearly the same. It eliminated the possibility that the 2500 Hz frequency band was affected by the glue bonded to the sensor.

In Figure 16, it could be observed that there were three significant vibration frequencies at high frequencies. Compared to Figure 14, the gearbox vibration test adopted an AB adhesive bonded sensor, the gearbox vibration amplitude measured by BK and Kistler sensors was similar, and the frequency characteristics were the same. It excluded the possibility that the 2500 Hz frequency band of gearbox vibration was caused by the sensor itself.

Gearbox vibration acceleration with Kistler sensor and 502 adhesive bonding is shown in Figure 15, and it could be

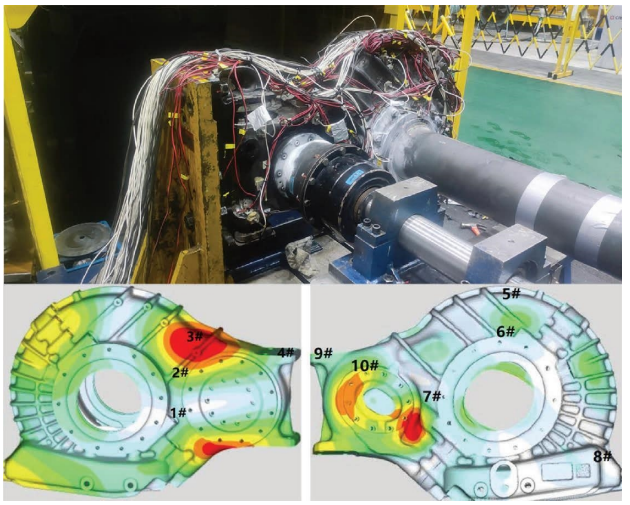

Figure 13: Site map of bench test and distribution position of measuring points for the gearbox.

seen that the vibration amplitude of three frequencies was clearly greater than that of the other vibration bands. Based on the comparative analysis of Figures 14–16, it can be seen that the gearbox had a significant resonance characteristic at about 2516 Hz, and the bonded sensor and bonded glue used in the gearbox vibration test had little effect on the gearbox vibration characteristic results.

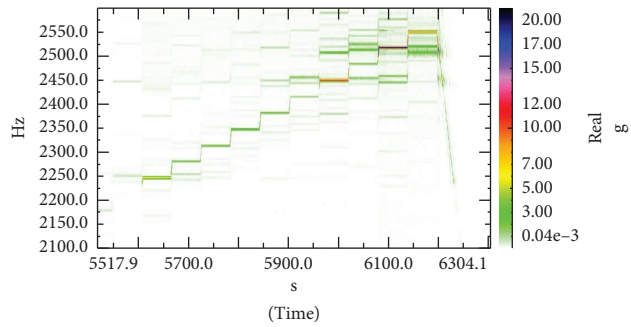

Figure 14: Time-frequency diagram of gearbox vibration acceleration with Kistler sensor and AB adhesive bonding.

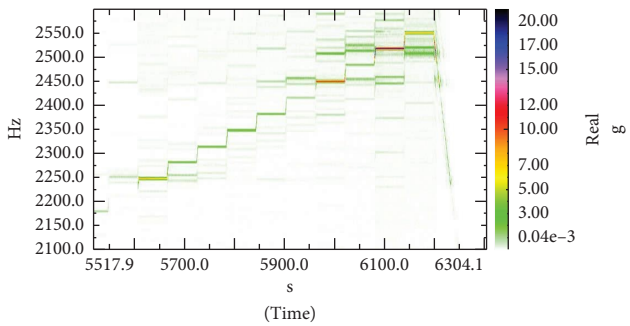

Figure 15: Time-frequency diagram of gearbox vibration acceleration with Kistler sensor and 502 adhesive bonding.

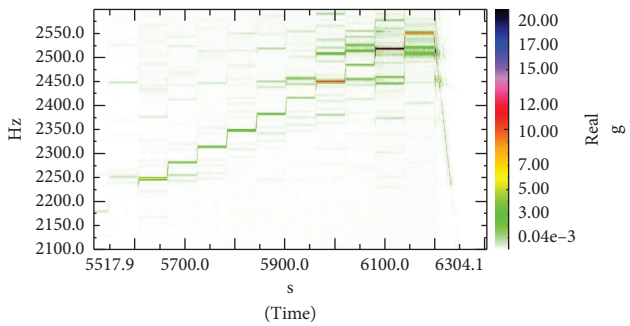

Figure 16: Time-frequency diagram of gearbox vibration acceleration with BK sensor and AB adhesive bonding.

4. Conclusions

With the rapid development of high-speed railways, the running speed of the train continues to improve, the dynamic characteristics of the vehicle are more complex, and the influence of the electrical part of the traction transmission system gradually appears. The on-site test results of the traction motor indicate that there is almost no significant gear meshing frequency band for the vibration acceleration of the motor within the corresponding gear meshing frequency band. During traction and braking, the traction motor vibration acceleration contains a very significant frequency component of 100 Hz, which is the beat frequency component formed from rectification. The simulation results indicate that the 100 Hz DC-link voltage pulsation would aggravate the fatigue damage of the motor hanger. The gearbox line test results show that there is a natural frequency of about 2500 Hz, and it was proved by the bench test of the gearbox.

Data Availability

The data used to support the findings of this study are available from the corresponding author upon request.

Conflicts of Interest

The authors declare that they have no conflicts of interest.

Authors' Contributions

P.W., X.W., S.Q., and H.W. conceived and investigated the study. S.Q. and C.S. conceived and supervised the study. P.W. and X.W. wrote the paper. All authors analyzed and discussed the results.

Acknowledgments

The financial support of the National Natural Science Foundation of China (U1934202) is gratefully acknowledged.

References

[1] K. Xu, J. Zeng, and L. Wei, "An analysis of the self-excited torsional vibration of high-speed train drive system," *Journal of Mechanical Science and Technology*, vol. 33, no. 3, pp. 1149–1158, 2019.

[2] H. T. Chen and B. Jiang, "A review of fault detection and diagnosis for the traction system in high-speed trains," *IEEE Transactions on Intelligent Transportation Systems*, vol. 21, no. 2, pp. 450–465, 2020.

[3] R. Li, J. Wang, X. Zhao, and X. Li, "Segmented power supply preset control method of high-speed rail contactless traction power supply system considering regenerative braking energy recovery," *Mathematical Problems in Engineering*, vol. 2020, Article ID 6698688, 15 pages, 2020.

[4] X. Wang, T. F. Peng, P. B. Wu, and L. T. Cui, "Influence of electrical part of traction transmission on dynamic characteristics of railway vehicles based on electromechanical coupling model," *Scientific Reports*, vol. 11, no. 1, Article ID 18409, 2021.

[5] H. Xia, N. Zhang, and Y. M. Cao, "Experimental study of train-induced vibrations of environments and buildings,"

Journal of Sound and Vibration, vol. 280, no. 3-5, pp. 1017–1029, 2005.

[6] D. Liu, T. Li, S. Meng, Z. Lu, and M. Zhong, "Investigating the car-body vibration of high-speed trains under different operating conditions with full-scale tests," *Vehicle System Dynamics*, vol. 60, no. 2, pp. 633–652, 2020.

[7] Y. F. Yang, L. Ling, C. Wang, Z. Q. Liu, K. Y. Wang, and W. M. Zhai, "Wheel/rail dynamic interaction induced by polygonal wear of locomotive wheels," *Vehicle System Dynamics*, vol. 60, no. 1, pp. 211–235, 2022.

[8] Z. W. Wang, W. H. Zhang, Z. H. Yin, Y. Cheng, G. H. Huang, and H. Y. Zou, "Effect of vehicle vibration environment of high-speed train on dynamic performance of axle box bearing," *Vehicle System Dynamics*, vol. 57, no. 4, pp. 543–563, 2019.

[9] G. H. Huang, N. Zhou, and W. H. Zhang, "Effect of internal dynamic excitation of the traction system on the dynamic behavior of a high-speed train," *Proceedings of the Institution of Mechanical Engineers-Part F: Journal of Rail and Rapid Transit*, vol. 230, no. 8, pp. 1899–1907, 2016.

[10] Q. Liu, T. Liang, and V. Dinavahi, "Real-time hierarchical neural network based fault detection and isolation for high-speed railway system under hybrid AC/DC grid," *IEEE Transactions on Power Delivery*, vol. 35, no. 6, pp. 2853–2864, 2020.

[11] C. Chang, L. Ling, Z. Han, K. Wang, and W. Zhai, "High-speed train-track-bridge dynamic interaction considering wheel-rail contact nonlinearity due to wheel hollow wear," *Shock and Vibration*, vol. 2019, Article ID 5874678, 18 pages, 2019.

[12] Y. Wu, X. Du, H. J. Zhang, Z. F. Wen, and X. S. Jin, "Experimental analysis of the mechanism of high-order polygonal wear of wheels of a high-speed train," *Journal of Zhejiang University-Science*, vol. 18, no. 8, pp. 579–592, 2017.

[13] Z. M. Chen, B. H. Zhang, B. Chen, and J. H. Fu, "Development and evaluation of torque distribution methods for four-wheel independent-drive electric vehicle based on parameter estimation," *Advances in Mechanical Engineering*, vol. 11, no. 5, Article ID 168781401984740, 2019.

[14] Z. W. Wang, G. M. Mei, Q. Xiong, Z. H. Yin, and W. H. Zhang, "Motor car-track spatial coupled dynamics model of a high-speed train with traction transmission systems," *Mechanism and Machine Theory*, vol. 137, pp. 386–403, 2019.

[15] H. Wu, P. B. Wu, K. Xu, J. C. Li, and F. S. Li, "Research on vibration characteristics and stress analysis of gearbox housing in high-speed trains," *IEEE Access*, vol. 7, pp. 102508–102518, 2019.

[16] Z. H. Yin, J. Y. Zhang, H. Y. Lu, and W. H. Zhang, "Dynamics modeling and analysis of a four-wheel independent motor-drive virtual-track train," *Proceedings of the Institution of Mechanical Engineers-Part K: Journal of Multi-body Dynamics*, vol. 235, no. 1, pp. 134–149, 2021.

[17] L. Y. Mao, W. J. Wang, Z. M. Liu, G. X. Yang, C. Y. Song, and S. Qu, "Research on causes of fatigue cracking in the motor hangers of high-speed trains induced by current fluctuation," *Engineering Failure Analysis*, vol. 127, 2021.

[18] P. B. Wu, J. Y. Guo, H. Wu, and J. Wei, "Influence of DC-link voltage pulsation of transmission systems on mechanical structure vibration and fatigue in high-speed trains," *Engineering Failure Analysis*, vol. 130, 2021.

[19] Y. Yao, Y. P. Yan, Z. K. Hu, and K. Chen, "The motor active flexible suspension and its dynamic effect on the high-speed train bogie," *Journal of Dynamic Systems, Measurement, and Control*, vol. 140, no. 6, 2018.

[20] H. W. Lee, C. B. Park, and J. Lee, "Improvement of thrust force properties of linear synchronous motor for an ultra-high-speed tube train," *IEEE Transactions on Magnetics*, vol. 47, no. 11, pp. 4629–4634, 2011.

[21] H. Zhu, Z. Zhu, P. Wu, C. Wang, Y. Yuan, and Q. Xu, "Vibration characteristics analysis of high-speed EMU gearbox housings under service conditions," *Noise and Vibration Control*, vol. 41, no. 2, pp. 15–20, 2021.

[22] Z. W. Wang, Z. H. Yin, P. Allen, R. C. Wang, Q. Xiong, and Y. M. Zhu, "Dynamic analysis of enhanced gear transmissions in the vehicle-track coupled dynamic system of a high-speed train," *Vehicle System Dynamics*, vol. 60, no. 8, pp. 2716–2738, 2022.

[23] Z. W. Wang, Y. Cheng, G. M. Mei, W. H. Zhang, G. H. Huang, and Z. H. Yin, "Torsional vibration analysis of the gear transmission system of high-speed trains with wheel defects," *Proceedings of the Institution of Mechanical Engineers-Part F: Journal of Rail and Rapid Transit*, vol. 234, no. 2, pp. 123–133, 2020.

[24] Z. S. Ren, X. Xin, G. Sun, and X. Wei, "The effect of gear meshing on the high-speed vehicle dynamics," *Vehicle System Dynamics*, vol. 59, no. 5, pp. 743–764, 2021.